Physics and Imaging in Radiation Oncology 28 (2023) 100506

Contents lists available at ScienceDirect

Physics and Imaging in Radiation Oncology

journal homepage: www.sciencedirect.com/journal/physics-and-imaging-in-radiation-oncology

Original Research Article

# Monte Carlo modelling of a prototype small-body portable graphite calorimeter for ultra-high dose rate proton beams

John Cotterill [a,*], Sam Flynn [a,b], Russell Thomas [a,c], Anna Subiel [a,d], Nigel Lee [a], David Shipley [a], Hugo Palmans [a,e], Ana Lourenço [a,d]

[a] Medical Radiation Science Group, National Physical Laboratory, Teddington TW11 0LW, UK
[b] Particle Physics Group, University of Birmingham, Edgbaston B15 2TT, UK
[c] University of Surrey, Faculty of Engineering and Physical Science, Guildford GU2 7XH, UK
[d] Department of Medical Physics and Biomedical Engineering, University College London, London WC1E 6BT, UK
[e] Medical Physics Group, MedAustron Ion Therapy Center, A-2700 Wiener Neustadt, Austria

ARTICLE INFO

*Keywords:*
Dosimetry
Proton
FLASH
UHDR
Monte Carlo
Calorimetry

ABSTRACT

*Background and purpose:* Accurate dosimetry in Ultra-High Dose Rate (UHDR) beams is challenging because high levels of ion recombination occur within ionisation chambers used as reference dosimeters. A Small-body Portable Graphite Calorimeter (SPGC) exhibiting a dose-rate independent response was built to offer reduced uncertainty on secondary standard dosimetry in UHDR regimes. The aim of this study was to quantify the effect of the geometry and material properties of the device on the dose measurement.

*Materials and methods:* A detailed model of the SPGC was built in the Monte Carlo code TOPAS (v3.6.1) to derive the impurity and gap correction factors, $k_{imp}$ and $k_{gap}$. A dose conversion factor, $D_w^{MC}/D_g^{MC}$, was also calculated using FLUKA (v2021.2.0). These factors convert the average dose to its graphite core to the dose-to-water for a 249.7 MeV mono-energetic spot-scanned clinical proton beam. The effect of the surrounding Styrofoam on the dose measurement was examined in the simulations by substituting it for graphite.

*Results:* The $k_{imp}$ and $k_{gap}$ correction factors were 0.9993 ± 0.0002 and 1.0000 ± 0.0001, respectively when the Styrofoam was not substituted, and 1.0037 ± 0.0002 and 0.9999 ± 0.0001, respectively when substituted for graphite. The dose conversion factor was calculated to be 1.0806 ± 0.0001. All uncertainties are Type A.

*Conclusions:* Impurity and gap correction factors, and the dose conversion factor were calculated for the SPGC in a FLASH proton beam. Separating out the effect of scatter from Styrofoam insulation showed this as the dominating correction factor, amounting to 1.0043 ± 0.0002.

## 1. Introduction

External beam radiotherapy is used in a significant proportion (approx. 50 %) of cancer treatments, either solely or in combination with other techniques [1]. These radiotherapy treatments are optimised such that the amount of radiation being delivered to the tumour is maximised, whilst minimising the radiation delivered to healthy tissue. A more recent development has been to deliver the radiation at Ultra-High Dose Rates (UHDR), often termed FLASH radiotherapy, to utilise the FLASH effect [2]. This effect has been observed to significantly spare healthy tissue through a mechanism that is not currently well understood, but still produces the same tumour killing effect as conventional dose-rate radiotherapy [3–6]. There has been significant progress made towards this modality as demonstrated by the first in human clinical trial using UHDR proton beams to treat symptomatic metastatic bone cancer [7,8].

Reference dosimetry is critical to maintain consistency between facilities of the dose delivered to a patient. This is important both on a national and international level to ensure a patient would receive the same dose, within an acceptable uncertainty, irrespective of the facility delivering the treatment. An International Code of Practice (TRS-398 [9]) published by the International Atomic Energy Agency (IAEA) recommends standard practices for facilities to follow, helping to keep them as consistent and accurate as possible. These standard practices

* Corresponding author at: Medical Radiation Science Group, National Physical Laboratory, Teddington TW11 0LW, UK.
*E-mail addresses:* john.cotterill@npl.co.uk (J. Cotterill), sam.flynn@npl.co.uk (S. Flynn), russell.thomas@npl.co.uk (R. Thomas), anna.subiel@npl.co.uk (A. Subiel), nigel.lee@npl.co.uk (N. Lee), david.shipley@npl.co.uk (D. Shipley), hugo.palmans@npl.co.uk (H. Palmans), ana.lourenco@npl.co.uk (A. Lourenço).

https://doi.org/10.1016/j.phro.2023.100506
Received 31 May 2023; Received in revised form 2 November 2023; Accepted 2 November 2023
Available online 8 November 2023

work well for the majority of currently employed techniques of performing external radiotherapy. However, at the increasingly utilised UHDR, these protocols are not adequate [10–12]. This is because ionisation chambers recommended for reference dosimetry in radiotherapy beams require a correction for ion recombination. This correction is small and linear as a function of dose rate or dose-per-pulse at the conventional dose rates typically employed clinically [13,14]. However, the amount of ion recombination significantly increases for UHDR modalities [14]. For some chambers, such as the PTW Roos and PTW Farmer chambers, this increase has been shown to result in a significantly larger ion recombination correction factor, exhibiting non-linear behaviour, and hence an increased uncertainty on the measured dose [10]. This larger uncertainty on dose can lead to an overdose to healthy tissue or insufficient dose for effective tumour control; both of which negatively impact the outcome for the patient.

National Metrology Institutes for Primary Standards of absorbed dose use calorimetry to directly measure the energy imparted per unit mass from a known amount of radiation [15,16]. The induced temperature rise due to ionising radiation in the calorimeter is measured and combined with the known specific heat capacity of the measuring medium to determine the absorbed dose. Correction factors are then applied to this value to derive the clinically relevant quantity of absorbed dose-to-water. The correction for heat transfer within the system is one of the main sources of uncertainty on the dose measurement when using calorimetry [16]. The uncertainty on the measurement therefore reduces with the increase in dose rate, as there is less time for heat to flow within the system during the shorter irradiation time [10]. This highlights that a calorimetric measurement of dose may offer a reduced uncertainty for UHDR beams, giving an improvement over the currently recommended ionisation chamber-based dosimetry.

A Small-body Portable Graphite Calorimeter (SPGC) [17] was developed by the National Physical Laboratory (NPL), UK, as a more compact, robust and simpler to operate device in comparison to its Primary-Standard Proton Calorimeter (PSPC) [16]. These advantageous characteristics mean it could be more easily used in different facilities to disseminate dose, as well as offer a reduced uncertainty on the measurement in comparison to ionisation chambers.

The clinically relevant quantity for dosimetry is dose-to-water, $D_w^m$, and can be derived according to the equation

$$D_w^m = \frac{D_w^{MC}}{D_g^{MC}} D_g^m \prod k_i,$$

where $D_g^m$ is the measured dose-to-graphite, $D_w^{MC}/D_g^{MC}$ is the Monte Carlo derived dose conversion factor, and $k_i$ represents additional correction factors. Two of the additional correction factors required in the conversion are the $k_{\text{imp}}$ and $k_{\text{gap}}$ correction factors. The $k_{\text{imp}}$ correction factor corrects for the non-graphite constituents of the calorimeter, such as core thermistors and impurities within the graphite itself. The $k_{\text{gap}}$ correction factor accounts for the presence of an air gap between the core and its surrounding jacket. The $D_w^{MC}/D_g^{MC}$ factor is then applied to convert the measured dose-to-graphite to the clinically relevant quantity of dose-to-water. This dose conversion factor is defined as the product of the water-to-graphite mass stopping power ratio, $s_{w,g}$, and the fluence correction factor, $k_{\text{fl}}$ [18]. These factors and corrections are always disseminated for the primary standard instruments maintained by the National Metrology Institutes. Several studies have been published demonstrating application of simplified calorimeters for UHDR dosimetry [11,19,20]. However, so far, no detailed evaluation of relevant correction factors for these instruments has been published. These corrections are instrumental in establishing these new devices as secondary standards for FLASH radiotherapy.

This work describes the Monte Carlo model and techniques used to derive the correction factors for the SPGC in a clinical UHDR proton beam. One of the simplifications of this device in comparison to the PSPC is that it is embedded in a Styrofoam phantom as opposed to a graphite phantom. This simplification results in a difference in the scattering conditions of the beam, as the surrounding phantom material is different to the core material of the calorimeter. The aim of this study was to examine the extent of this difference in scatter, and therefore dose to the calorimeter core. This motivated the introduction of a separate $k_{\text{scat}}$ correction factor.

## 2. Materials and methods

### 2.1. Small-body Portable Graphite Calorimeter

The SPGC used constituted a 2 mm thick graphite core of 20 mm diameter, enclosed in a graphite jacket. An air gap was present between the core and jacket to minimise the heat transfer between the components during irradiation. Thermistors were present in the core to measure its temperature, and consequently the temperature rise when irradiated. The jacket, containing the core, was then embedded in Styrofoam to improve the thermal isolation of the graphite from the environment. This geometry, modelled in TOPAS, is shown in Fig. 1.

### 2.2. Simulation model

The geometry of the calorimeter was modelled in TOPAS (v3.6.1), based on Geant4 v10.6.p03 [21,22]. Simulations were performed with the default reference physics lists, including g4h-phy_QGSP_BIC_HP for hadronic physics and g4em-standard_opt4 for electromagnetic physics [23]. The graphite materials were defined with a measured density of 1.767 g • cm$^{-3}$ [17], measured at NPL, and an ionisation potential of 81 eV in accordance with the recommendations in International Commission on Radiation Units and Measurements Report 90 [24]. The impurities of the graphite were defined based on an example impurity analysis from a manufacturer of the same quality graphite. The Styrofoam material was defined with the density of 0.0392 g • cm$^{-3}$ measured at NPL [17], and an ionisation potential of 68.7 eV as defined for polystyrene by the National Institute of Standards and Technology (NIST) [25]. The elemental composition was also defined in accordance with the NIST database.

Individual thermistors were modelled to ensure the most accurate proportion of non-graphite materials were included in the calorimeter model. This intricate modelling allowed for the potential of reduced Type B uncertainties on the $k_{\text{imp}}$ correction factor. Dimensions and elemental compositions were taken from specification documents from the manufacturer.

### 2.3. Geometry configurations

The core in NPL's PSPC is surrounded by a series of vacuum gaps and graphite jackets. This means that the proton scatter into the core is relatively consistent because of the similarity of the surrounding material. However, the more simplistic design of the SPGC with surrounding Styrofoam introduced a difference in the amount of proton scatter in comparison to homogeneous graphite. The effect of substituting the Styrofoam for graphite was therefore examined for this study.

The configurations of the simulation model were:

a) Full geometry: containing impure graphite and non-graphite components.

bi) Pure graphite geometry: impure graphite and non-graphite components were substituted for pure graphite. The air gap and Styrofoam phantom remained present.

bii) Pure graphite geometry: impure graphite and non-graphite components were substituted for pure graphite. The air gap remained present. The Styrofoam phantom was substituted for a pure graphite

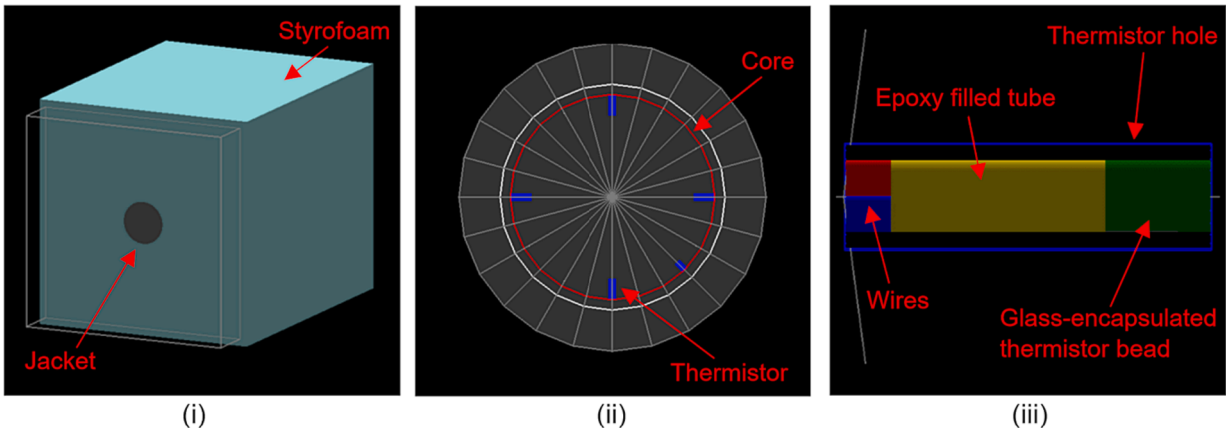


**Fig. 1.** TOPAS model of the Small-body Portable Graphite Calorimeter. (i) Graphite jacket, containing graphite core, surrounded by Styrofoam. (ii) Graphite jacket showing the position of the core and core thermistors. (iii) Individual thermistor model.

phantom.

ci) Compensated geometry: the air gap surrounding the core was shifted downstream and filled with pure graphite to make the material homogeneous. This maintained the same amount of graphite in front of the core. The Styrofoam phantom remained present.

cii) Compensated geometry: the air gap surrounding the core was shifted downstream and filled with pure graphite to make the material homogeneous. This maintained the same amount of graphite in front of the core. The Styrofoam phantom was substituted for a pure graphite phantom.

Configurations a, bi and ci are shown in Fig. 2. Configurations bii and cii had the same geometries as bi and ci, except the Styrofoam phantom was substituted for a pure graphite phantom.

### 2.4. Correction factor calculations

The $k_{imp}$ and $k_{gap}$ correction factors were calculated as the ratio of dose scored within the core regions in the different configurations. The $k_{imp}$ correction factor, being the ratio between the pure graphite geometry and full geometry, converts the dose-to-core in the full geometry to the dose-to-core in pure graphite. The $k_{gap}$ correction factor is the ratio between the compensated geometry and the pure graphite geometry, which converts the dose-to-core in pure graphite (containing air gaps), to the dose-to-core in homogeneous pure graphite (no air gaps). These correction factors were calculated for both pathways, the first with the Styrofoam phantom remaining present (configurations a, bi, ci), and the second when the Styrofoam phantom was substituted for a pure graphite phantom (configurations a, bii, cii).

The dose conversion factor has been found to largely depend on the nuclear models used in the Monte Carlo code and, as shown in [18], is not (or only very weakly) correlated with other interaction data such as energy loss and scatter. This justified the use of a different code which could better model the nuclear interactions. It was for this reason that the simulations for the dose conversion factor were instead conducted with FLUKA (v2021.2.0), using the default HADROTHErapy card [26]. Previous work has demonstrated good agreement between experimentally derived and simulated partial fluence correction factors using the code [27] and we observed that with Geant4, not the same level of agreement could be achieved. The dose conversion factor was determined by scoring the dose as a function of depth in both pure homogeneous graphite and water. The depth-dose curve in pure homogeneous graphite was then scaled such that its range matched that in water, giving a dose at a water equivalent depth. The ratio in dose at the required depth of 5.2 g • $cm^{-2}$ used experimentally then gave the dose conversion factor.

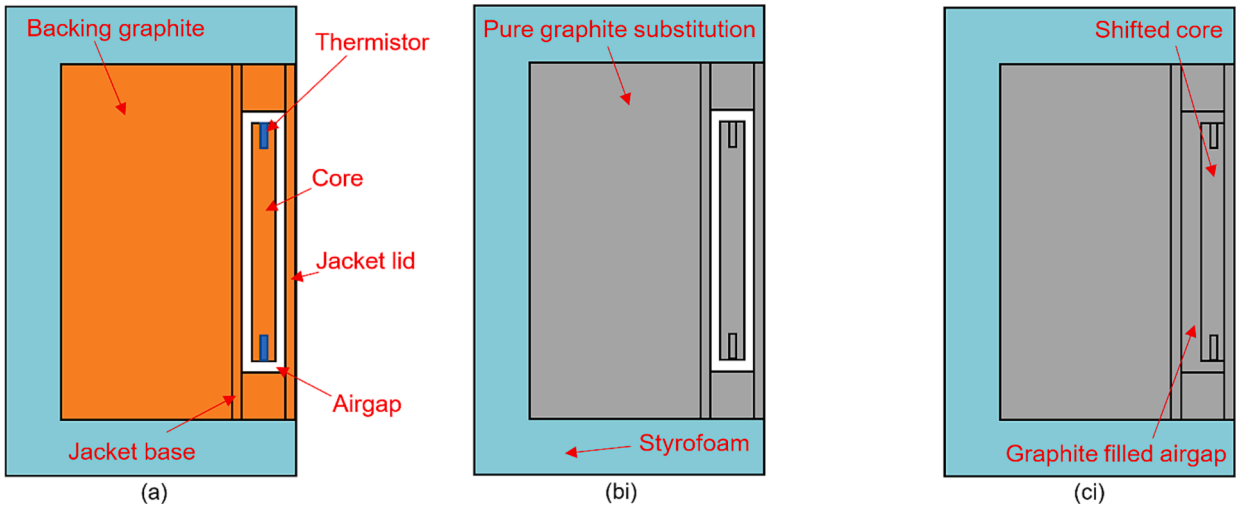


**Fig. 2.** Schematic diagrams of the (a) full geometry with impure graphite and non-graphite materials, (bi) pure graphite geometry in a Styrofoam phantom, and (ci) compensated geometry in a Styrofoam phantom.

### 2.5. Beam model

All geometries were simulated using a 249.7 MeV spot-scanned proton beam, with a Gaussian energy spread (standard deviation) of 0.25 MeV, over a 5 cm × 6 cm field area, with divergence of 3.5 mrad. These beam specifications were based on Monte Carlo optimised beam parameters from an experimental campaign conducted at Cincinnati Children's Hospital Medical Center [10]. The proton energy, energy spread, field dimensions and divergence of the beam were optimised using experimentally obtained percentage depth-dose data, and beam profiles measured using Gafchromic EBT3 films. The dose rate was not required to be simulated as the correction factors are only dependent on the spatial distribution of the beam, and not on the dose rate or dose-per-pulse [28].

## 3. Results

The values of the $k_{imp}$ and $k_{gap}$ correction factors without substitution of the Styrofoam phantom were calculated to be 0.9993 ± 0.0002 and 1.0000 ± 0.0001, respectively. The correction factors where the Styrofoam phantom had been substituted for a pure graphite phantom were 1.0037 ± 0.0002 and 0.9999 ± 0.0001, respectively. The dose conversion factor, $D_w^{MC}/D_g^{MC}$, was calculated to be 1.0806 ± 0.0001. The quoted uncertainties are Type A uncertainties and refer to the standard error of the mean.

## 4. Discussion

The results showed little difference between the $k_{gap}$ correction factors irrespective of the Styrofoam substitution to graphite (<0.1 % difference). However, there was found to be a larger difference between the $k_{imp}$ correction factors calculated (0.44 % increase). The substitution of the Styrofoam for the higher density pure graphite resulted in more protons being scattered into the core. This increase in protons increased the dose received by the core, and consequently increased the $k_{imp}$ correction factor. This showed that the scatter of the protons from the surrounding phantom material of the calorimeter had a significant impact on the derived $k_{imp}$ correction factor, and benefited from being separately considered.

A scattering correction factor, $k_{scat}$, was introduced as an alternative to the substitution of Styrofoam to graphite when calculating the $k_{imp}$ correction factor. In this way, the $k_{imp}$ correction factor only corrected for the impurities and non-graphite materials within the core, and therefore was more comparable to the equivalent PSPC correction factor [10]. The $k_{scat}$ correction factor was then separately implemented to correct for the scatter into the core from the surrounding phantom material. Separation of these effects is valuable for future design studies, as well as comparing the response with ionisation chambers in a full-scatter graphite or water phantom.

In the case of the SPGC with this alternative formulation, the $k_{imp}$ correction factor was 0.9993 ± 0.0002, which converted the dose-to-core to a dose-to-core in pure graphite (considering internal impurities). A $k_{scat}$ correction factor of 1.0043 ± 0.0002 then converted the dose-to-core in pure graphite (considering internal impurities) to a dose-to-core in pure graphite (considering the external phantom material). Finally, the $k_{gap}$ correction of 0.9999 ± 0.0001 was applied to convert to the dose-to-core in homogeneous pure graphite. The $D_w^{MC}/D_g^{MC}$ correction factor, converting to dose-to-water, was found to be comparable with previously reported values [10].

There are additional Type B uncertainty components to be applied to the $k_{imp}$ and $k_{gap}$ correction factor values which are associated with uncertainties on the geometry description, the optimised beam source characteristics, and the radiation transport modelling used by the Monte Carlo code. The uncertainties on the interaction data used in the modelling may also have influenced these results, such as the uncertainty on the mean excitation energy of graphite, and the uncertainties on the nuclear interaction cross sections. The latter has particular importance as this study considered the impact of scatter from the surrounding phantom material on the dose to the core of the calorimeter. It is also important for determining how the dose is deposited in a material, and therefore would impact the dose conversion factor calculation. These uncertainties are subject to further analysis when detailed comparison with experimental data is completed.

The reference dosimetry for UHDR proton beams is challenging. Typically used ionisation chambers suffer from large ion recombination effects which increase the uncertainty on the dose they measure. The detailed modelling of NPL's SPGC using Monte Carlo has allowed for improved quantification of the scattering effects occurring within the device. Unlike the PSPC, the SPGC was surrounded by Styrofoam which impacted the scattering of protons into the core. A $k_{scat}$ correction factor has been introduced to account for the influence of the surrounding phantom material on the dose measured in the core of the calorimeter.

A device like the SPGC, given its dose rate independent response [29], is likely to offer a reduced uncertainty on the measured dose for reference dosimetry in UHDR beams in comparison to ionisation chambers. This reduces the uncertainty on the dose delivered to the tissues of a patient, and the uncertainty on the Normal Tissue Complication Probability, which is beneficial for patient outcome [30]. The improved quantification of the scattering effects occurring within the SPGC described in this study, and the calculated correction factors required to obtain dose-to-water, brings use of the device closer to the fore. This development of the reference dosimetry is critical to keep the rapidly developing UHDR techniques in radiotherapy safe and accurate for patients.

It is envisioned that a device such as the SPGC be used to disseminate dose in FLASH facilities as an alternative to ionisation chambers, especially in pulsed UHDR beams where ion recombination effects are highly pronounced. Its portability and relative simplicity in comparison to the PSPC means routine use in facilities would be possible. Its clinical benefit also spans beyond UHDR proton treatment facilities, as UHDR electron and x-ray treatment facilities may also benefit. This instrument is therefore a building block necessary for development of clinical calorimeters which could be routinely used for dosimetry in UHDR radiotherapy. There is further potential for such an instrument to be used as an auditing device, which can be transported between facilities for intercomparison measurements. This could help to improve the standardisation of UHDR treatments nationally and globally, enabling consistency across different facilities and comparability of results.

To conclude, the compact SPGC device may offer a reduced uncertainty on measurements for reference dosimetry in UHDR proton beams. The simplified geometry of the device which utilised a Styrofoam phantom surrounding the graphite components caused differences in the scatter conditions of the protons in comparison to a uniform material. This difference in the scatter lead to an impact on the dose measurement. The extent of this impact was examined using Monte Carlo and accounted for in a $k_{scat}$ correction factor equal to 1.0043 ± 0.0002 for the SPGC in the set up described.

## CRediT authorship contribution statement

**John Cotterill:** Methodology, Software, Validation, Formal analysis, Data curation, Writing – original draft, Writing – review & editing, Visualization. **Sam Flynn:** Software, Validation, Formal analysis. **Russell Thomas:** Conceptualization, Investigation, Resources, Supervision, Funding acquisition. **Anna Subiel:** Conceptualization, Investigation, Supervision, Project administration. **Nigel Lee:** Investigation, Resources. **David Shipley:** Methodology, Software, Validation, Formal analysis, Resources. **Hugo Palmans:** Conceptualization, Methodology, Validation, Formal analysis. **Ana Lourenço:** Conceptualization, Methodology, Validation, Formal analysis, Investigation, Supervision, Project administration, Funding acquisition.

## Declaration of Competing Interest

The authors declare that they have no known competing financial interests or personal relationships that could have appeared to influence the work reported in this paper.

## References


[1] Delaney G, Jacob S, Featherstone C, Barton M. The role of radiotherapy in cancer treatment: estimating optimal utilization from a review of evidence-based clinical guidelines. Cancer 2005;104:1129–37. https://doi.org/10.1002/cncr.21324. Erratum in: Cancer. 2006;107:660.

[2] Hughes JR, Parsons JL. FLASH radiotherapy: current knowledge and future insights using proton-beam therapy. Int J Mol Sci 2020;21:6492. https://doi.org/10.3390/ijms21186492.

[3] Favaudon V, Caplier L, Monceau V, Pouzoulet F, Sayarath M, Fouillade C, et al. Ultrahigh dose-rate FLASH irradiation increases the differential response between normal and tumor tissue in mice. Sci Transl Med 2014;6:245ra93. https://doi.org/10.1126/scitranslmed.3008973.

[4] Montay-Gruel P, Petersson K, Jaccard M, Boivin G, Germond JF, Petit B, et al. Irradiation in a flash: Unique sparing of memory in mice after whole brain irradiation with dose rates above 100Gy/s. Radiother Oncol 2017;124:365–9. https://doi.org/10.1016/j.radonc.2017.05.003.

[5] Vozenin MC, Fornel PD, Petersson K, Favaudon V, Jaccard M, Germond JF, et al. The Advantage of FLASH Radiotherapy Confirmed in Mini-pig and Cat-cancer Patients. Clin Cancer Res 2019;25:35–42. https://doi.org/10.1158/1078-0432.CCR-17-3375.

[6] Bourhis J, Sozzi WJ, Jorge PG, Gaide O, Bailat C, Duclos F, et al. Treatment of a first patient with FLASH-radiotherapy. Radiother Oncol 2019;139:18–22. https://doi.org/10.1016/j.radonc.2019.06.019.

[7] Daugherty EC, Mascia A, Zhang Y, Lee E, Xiao Z, Sertorio M, et al. FLASH radiotherapy for the treatment of symptomatic bone metastases (FAST-01): protocol for the first prospective feasibility study. JMIR Res Protoc 2023;12:e41812. https://doi.org/10.2196/41812.

[8] Daugherty EC, Mascia AE, Sertorio MGB, Zhang Y, Lee E, Xiao Z, et al. FAST-01: Results of the First-in-Human Study of Proton FLASH Radiotherapy. Int J Radiat Oncol Biol Phys 2022;114:S4 Supplement. https://doi.org/10.1016/j.ijrobp.2022.07.2325.

[9] Andreo P, Burns DT, Hohlfeld K, Huq MS, Kanai T, Laitano F, et al. Absorbed dose determination in external beam radiotherapy: An international code of practice for dosimetry based on standards of absorbed dose to water. IAEA Technical Report Series. 2000;TRS-398.

[10] Lourenço A, Subiel A, Lee N, Flynn S, Cotterill J, Shipley D, et al. Absolute dosimetry for FLASH proton pencil beam scanning radiotherapy. Sci Rep 2023;13:2054. https://doi.org/10.1038/s41598-023-28192-0.

[11] McManus M, Romano F, Lee ND, Farabolini W, Gilardi A, Royle G, et al. The challenge of ionisation chamber dosimetry in ultra-short pulsed high dose-rate very high energy electron beams. Sci Rep 2020;10:9089. https://doi.org/10.1038/s41598-020-65819-y.

[12] Kranzer R, Poppinga D, Weidner J, Schuller A, Hackel T, Looe HK, et al. Ion collection efficiency of ionization chambers in ultra-high dose-per-pulse electron beams. Med Phys 2021;48:819–30. https://doi.org/10.1002/mp.14620.

[13] Palmans H, Seuntjens J, Verhaegen F, Denis JM, Vynckier S, Thierens H. Water calorimetry and ionisation chamber dosimetry in an 85-MeV clinical proton beam. Med Phys 1996;23:643–50. https://doi.org/10.1118/1.597700.

[14] Palmans H, Thomas R, Kacperek A. Ion recombination correction in the Clatterbridge Centre of Oncology clinical proton beam. Phys Med Biol 2006;51:903–17. https://doi.org/10.1088/0031-9155/51/4/010.

[15] Renaud J, Palmans H, Sarfehnia A, Seuntjens J. Absorbed dose calorimetry. Phys Med Biol 2020;65:05TR02. https://doi.org/10.1088/1361-6560/ab4f29.

[16] Lourenço A, Lee N, Shipley D, Romano F, Kacperek A, Duane S, et al. Application of a portable primary standard level graphite calorimeter for absolute dosimetry in a clinical low-energy passively scattered proton beam. Phys Med Biol 2022;67:225021. https://doi.org/10.1088/1361-6560/ac95f6.

[17] Palmans H, Thomas R, Simon M, Duane S, Kacperek A, DuSautoy A, et al. A small-body portable graphite calorimeter for dosimetry in low-energy clinical proton beams. Phys Med Biol 2004;49:3737–49. https://doi.org/10.1088/0031-9155/49/16/019.

[18] Palmans H, Al-Sulaiti L, Andreo P, Shipley D, Luhr A, Bassler N, et al. Fluence correction factors for graphite calorimetry in a low-energy clinical proton beam: I. Analytical and Monte Carlo simulations. Phys Med Biol 2013;58:3481–99. https://doi.org/10.1088/0031-9155/58/10/3481.

[19] Renaud J, Sarfehnia A, Bancheri J, Seuntjens J. Aerrow: A probe-format graphite calorimeter for absolute dosimetry of high-energy photon beams in the clinical environment. Med Phys 2018;45:414–28. https://doi.org/10.1002/mp.12669.

[20] Bourgouin A, Knyziak A, Marinelli M, Kranzer R, Schüller A, Kapsch RP. Characterization of the PTB ultra-high pulse dose rate reference electron beam. Phys Med Biol 2022;67:085013. https://doi.org/10.1088/1361-6560/ac5de8.

[21] Perl J, Shin J, Schümann J, Faddegon B, Paganetti H. TOPAS: an innovative proton Monte Carlo platform for research and clinical applications. Med Phys 2012;39:6818–37. https://doi.org/10.1118/1.4758060.

[22] Faddegon B, Ramos-Méndez J, Schuemann J, McNamara A, Shin J, Perl J, et al. The TOPAS tool for particle simulation, a Monte Carlo simulation tool for physics, biology and clinical research. Phys Med 2020;72:114–21. https://doi.org/10.1016/j.ejmp.2020.03.019.

[23] TOPAS MC Inc. TOPAS Documentation: Release 3.7. 2021. https://topas.readthedocs.io/_/downloads/en/3.7.0/pdf/ [accessed 24 October 2023].

[24] International Commission on Radiation Units and Measurements. Key Data for Ionizing-Radiation Dosimetry: Measurement Standards and Applications. ICRU Report No 90. 2016.

[25] Berger MJ, Coursey JS, Zucker MA, Chang J. NIST Standard Reference Database 124. National Institute of Standards and Technology. Last Update to Data Content. 2017. https://doi.org/10.18434/T4NC7P.

[26] Ferrari A, Sala PR, Fasso A, Ranft J. Fluka: a multi-particle transport code. 2023; Revision 156. http://www.fluka.org/content/manuals/FM.pdf [accessed 24 October 2023].

[27] Lourenço A, Thomas R, Bouchard H, Kacperek A, Vondracek V, Royle G, et al. Experimental and Monte Carlo studies of fluence corrections for graphite calorimetry in low- and high-energy clinical proton beams. Med Phys 2016;43:4122–32. https://doi.org/10.1118/1.4951733.

[28] Subiel A, Romano F. Recent developments in absolute dosimetry for FLASH radiotherapy. Br J Radiol 2023;96:20220560. https://doi.org/10.1259/bjr.20220560.

[29] Romano F, Bailat C, Jorge PG, Lerch MLF, Darafsheh A. Ultra-high dose rate dosimetry: Challenges and opportunities for FLASH radiation therapy. Med Phys 2022;49:4912–32. https://doi.org/10.1002/mp.15649.

[30] Van den Bosch L, Schuit E, Paul van der Laan H, Reitsma JB, Moons KGM, Steenbakkers RJHM, et al. Key challenges in normal tissue complication probability model development and validation: towards a comprehensive strategy. Radiother Oncol 2020;148:151–6. https://doi.org/10.1016/j.radonc.2020.04.012.